First High-Resolution Infrared Spectra of 2-^{13}C-Propane

Analyses of the ν_{26} (B_2) c-Type and ν_9 (A_1) b-Type Bands

Stephen J. Daunt* and Robert Grzywacz

Department of Physics & Astronomy, The University of Tennessee, Knoxville, TN

Colin M. Western*

School of Chemistry, University of Bristol, Bristol, UK

Walter J. Lafferty†

Optical Technology Division, NIST, Gaithersburg, MD

Jean-Marie Flaud

Universités Paris Est Créteil et Paris Diderot, LISA, Créteil, France

Brant E. Billinghurst

Canadian Light Source, University of Saskatchewan, Saskatoon, SK, Canada

Richard Hutchings

ICON Isotopes/Berry & Associates, Dexter, MI

† Deceased December 27, 2018

Corresponding authors: sdaunt@utk.edu or C.M.Western@bristol.ac.uk

Abstract

This paper presents the first high resolution ($\Delta\nu$ = 0.00096 cm^{-1}) IR investigation of 2-^{13}C-propane. Spectra of the $\nu_9(A_1)$ CCC skeletal bending mode near 336.767 cm^{-1} (a b-type band) and the $\nu_{26}(B_2)$ methylene (CH_2) rocking mode near 746.614 cm^{-1} (a c-type band) were recorded at the Canadian Light Source (CLS) synchrotron. The spectra were assigned both traditionally and with the aid of the PGOPHER program. As only limited microwave data are available for this molecule the present data was used to determine a new set of ground state constants that included centrifugal distortion terms. Upper state constants for both bands have been determined that provide a good simulation of the spectra. The analysis also included the strong a-type Coriolis resonance between the ν_{26} and $2\nu_9$ states that causes strong perturbation-allowed transitions to appear in the spectrum. Lines of the $2\nu_9$-ν_9 hot band were also assigned and included in our analysis of the bending region. This data will be useful in identifying isotopic propane lines in Titan and other astrophysical objects.

Introduction

The Voyager discovery of propane on Titan [1] is an excellent illustration of the importance of high-quality infra-red spectra for astronomy. The Titan observation prompted a FT-IR study [2] at the Kitt Peak National Observatory (KPNO), though as improved spacecraft and ground-based astronomical observations were made [3, 4] in the following years it became clear that laboratory data of better resolution as well as a more detailed analysis was required. This prompted several studies of propane [5-7], and recent articles by Perrin *et al*. [8, 9] summarize the several high-resolution studies that have been done that support investigation of Titan and NASA missions (Voyager, Galileo & Cassini) to the outer Solar System. The infra-red work has also been used to study propane that has also been found on Jupiter and Saturn[10-13]. The IR bands have also been used for other satellite, aircraft and ground-based telescopic observations [3, 4]. Intensity, temperature and collision broadening studies have also been done recently to aid in the astrophysical studies [14-16]. The interstellar medium where new solar systems exist or are forming is also a place to expect to find propane since other organic molecules have been detected by these same observing methodologies [17].

Propane is also important in terrestrial studies and is the second most abundant non methane hydrocarbon in the Earth's atmosphere. C_2 to C_{10} hydrocarbons from car exhausts have been identified as precursors to the formation of street-level ozone and urban smog. North American, European, and other regulators require round-the-clock monitoring of these compounds in major urban areas[18, 19], particularly during the summer months when sunlight is most intense. In addition, regulations developed in response to the Kyoto protocol on greenhouse gases require the monitoring of trace-level ultra-volatile compounds with global warming and ozone-depleting potential. In both terrestrial and extra-terrestrial studies measurement of isotopic ratios and isotopically labelled tracers give invaluable information on the past history and sources of these compounds. For example, with the rising use of propane as a more significant fuel source and the increasing development of fracking as a source of gases (which include propane) there have been many recent studies of C and H isotopic fractionation of hydrocarbons and CO_2 during gas desorption from coal and shale[20]. The study of ^{13}C ratios has even been suggested as a way of evaluating the age and quality of shale deposits in the geochemical literature [21, 22].

Determination of isotopic ratios from infrared spectroscopy requires line lists or models of isotopologues to be of as good quality as that of the main isotopologue, but this is where the available literature is very limited. There have been a series of low- to moderate-resolution studies establishing the vibrational assignment and force field for propane, starting with a series of papers by Henry L. McMurry and colleagues [23-26] and others [27] on the low-resolution IR spectra of various deuterated propanes. Later work includes further IR spectra and force field analyses by Gayles *et al*[28, 29] and Pearce and Levin[30]. A thorough series of Raman studies of many deuterated species of propane, also including a force field analysis, was performed by Murphy, Gough and co-workers [31-33]. There was also a band intensity study by Kondo and Saëki [34], of normal propane, $CH_3CD_2CH_3$ and $CD_3CH_2CD_3$ and a cross-section study of 1-^{13}C-propane by Loh and Wolff [35] in the C-H stretching region. The only pure rotational work is microwave spectra by Lide in 1960 [36], who recorded six pure rotational microwave transitions for 1-^{13}C-propane, 2-^{13}C-propane and three singly substituted deuterium isotopologues. These yielded the three main rotational constants (*A*, *B* and *C*) but none of the centrifugal distortion constants.

There were early attempts to calculate propane band intensities for some deuterated propanes with *ab initio* methods by Blom and Altona[37] and for the normal species of alkanes by Fischer *et al* [38]. More recently a high-quality set of *ab initio* calculations has been published predicting frequencies, inertial defects and

centrifugal distortion constants for the singly substituted deuterium and ^{13}C isotopic species of propane [39], but these will require experimental validation through high-resolution spectroscopy to be useful.

We have thus begun a series of measurements with the aim of providing high-quality line lists for several D and ^{13}C substituted isotopologues of propane with the eventual goals of having these analyses incorporated into the international spectral databases of GEISA[40] and HITRAN[41]. In this initial study the symmetrical 2-^{13}C-propane is chosen as this is likely to be the most straightforward to analyze, given the symmetry is the same as the main isotopologue (implying no hybrid bands) and there is only one possible isomer.

The Titan work on the main isotopologue of propane has mainly concentrated[4] on the ν_{26} band of the at 748.5 cm^{-1}, as this is spectroscopically the most tractable. However, even for this band the analysis is not entirely straightforward. The first high-resolution study using the KPNO data [2] indicated the band was perturbed for $K_a' > 14$ because of a resonance with an overtone of the ν_9 skeletal bending. The spectra were not sufficiently resolved in this study (0.005 cm^{-1}) near the band center to be definitively assigned, limiting the quality of the resulting model and its applicability to the improving astronomical data. Subsequent higher (0.00096 cm^{-1}) resolution work[5] confirmed the presence of perturbation, which was found to be a strong a-type Coriolis interaction between ν_{26} and $2\nu_9$. This analysis was significantly aided by simultaneous analysis of the $2\nu_9-\nu_9$ hot band at 740.292 cm^{-1}, as this allowed most levels of $2\nu_9$ to be observed directly, rather than just those strongly mixed with ν_{26}. The ν_9 fundamental at 369.223 cm^{-1} was subsequently analyzed[6], and found to be unperturbed. For propane internal rotation is potentially important, given the presence of two low-frequency torsional modes at 217 cm^{-1} and 265 cm^{-1}, first measured by inelastic neutron scattering[42]. This implies significant intensity for hot bands involving these modes, given that the $2\nu_9-\nu_9$ hot band has been analyzed as mentioned above. Fortunately from the analysis point of view the ground state, ν_9, $2\nu_9$ and ν_{26} do not show any torsional splittings, though other states do, significantly complicating their analysis[8, 9].

For this initial study we therefore concentrate on the ν_{26} and ν_9 regions for 2-^{13}C-propane, making use the high-resolution (0.00096 cm^{-1}) Fourier transform spectra available from the far IR beam line of the Canadian Light Source[43]. We present a simultaneous analysis using the PGOPHER program[44] of the ν_9, ν_{26} and $2\nu_9-\nu_9$ bands, sufficient to reproduce all the assigned bands to an accuracy of better than 0.0002 cm^{-1}. As part of this ground state constants are also determined by a combination difference fit, given the lack of available information on centrifugal distortion. A preliminary version of this analysis was reported at the 2017 International Symposium on Molecular Spectroscopy (ISMS)[45].

Experimental

Synthesis of 2-^{13}C- Propane

2-^{13}C-propane was not commercially available, so a synthesis was performed by RH. As this is not a typical procedure we give the details here.

All reactions were run in anhydrous solvents under dry argon. Commercial reagents were used as received. 2-^{13}C-2-Bromopropane (99 atom%) was prepared from 2-^{13}C-2-propanol according to the procedure of Kozlowski *et al* [46]. An oven dried 250 mL, three-neck flask equipped with a stir bar, reflux condenser, rubber septa, and a gas adaptor was charged with magnesium turnings (3.2 g, 135 mmol). The flask was evacuated and backfilled with argon *via* an inlet adapter attached to the top of the reflux condenser. The flask was charged with anhydrous diethylene glycol dimethyl ether (100 mL) and the solvent was degassed by cooling to 0°C, pumping under high vacuum, and back filling with argon (3X). A crystal of iodine and 2-^{13}C-2-bromopropane (4.0 g, 32 mmol) were added to the flask, and the mixture was warmed under argon with a heating mantle to initiate a reaction. When the iodine color was gone, the remaining 2-^{13}C-2-bromopropane (10.0 g, 80 mmol) was added in portions so as to maintain a gentle reflux. Upon complete

addition of 2-^{13}C-2-bromopropane the reaction mixture was allowed to cool to ambient temperature and stirred for approximately 1 h. The inlet adaptor was connected with Tygon tubing to a gas train consisting of a small vacuum trap, a Schwartz tube, and a mineral oil bubbler; the vacuum trap and Schwartz tube being evacuated and back filled with argon prior to attaching the bubbler. The entire train was then open to the reaction flask with argon flowing through the condenser to the bubbler. The vacuum trap was placed in a cooling bath at -30 °C (40% methanol-methanol/dry ice) and the Schwarz tube was placed in a cooling bath cooled to -89 °C (*i*-PrOH/Liq.N_2) taking care to maintain a positive flow of argon. Deionized water (4.0 mL, excess) was slowly added, via syringe, to the reaction mixture over a period of 20 minutes at a rate that maintained a steady flow of gas as indicated by the mineral oil bubbler. Over this time, the reaction mixture becomes warm and 2-^{13}C-propane was collected in the Schwarz tube. After the addition of water was complete, propane-2-^{13}C was isolated from the reaction apparatus and carefully vacuum distilled to a second Schwarz tube cooled in a bath at -89 °C (*i*-PrOH/Liq.N_2). The product was finally vacuum transferred to an evacuated lecture bottle for storage. The overall yield of 2-^{13}C-propane was 2.79 g (55%).

Purity was first checked by taking ^{1}H spectra recorded with an Agilent spectrometer working at 400 MHz. [^{1}H NMR (400 MHz, $CDCl_3$): δ 1.30 (doublet of septets, 2H, $J_{C,H}$ = 124 Hz, $J_{H,H}$ = 7.2 Hz), 0.88 (dt, 6H, $J_{C,H}$ = 4.5 Hz, $J_{H,H}$ = 7.2 Hz); Chemical shifts (δ) are expressed in parts per million (ppm) from tetramethylsilane.] The 2-^{13}C-propane sample was analyzed using a Wilmad® quick pressure valve NMR tube. Enrichment at C-2 was 99 atom% based on the starting material. The product contained approximately 3.8% 2-^{13}C-propene based on the ^{1}H NMR data.

CLS Far-IR Synchrotron Spectra

All the spectra discussed in this paper were recorded with a Bruker 125HR FTS at the Canadian Light Source Synchrotron Far-IR beamline during Cycle 22 (Aug-Sep, 2015). The data analyzed here were all recorded at a resolution of 0.00096 cm^{-1}. At that time the instrument was using a liquid Helium cooled Cu:Ge detector. The samples were contained in a 2 m White type cell set for an optical path length of 72 m. The White cell could be cooled by a recycling refrigerated liquid coolant system.

The ν_{26} spectra were recorded at room temperature (296 ± 1K) with a pressure of 0.065 Torr in the White cell, using a KBr beam splitter and an entrance aperture of 1.15 mm. The analyzed spectrum was computed by averaging 368 scans. The calibration of the spectra were checked using residual lines from the ν_2 band of CO_2 in the spectrometer against the HITRAN[41] database. This suggested a possible shift to lower frequency of our values of 0.0002 cm^{-1} was required, but as this is close to our measurement accuracy, and the accuracy of the HITRAN values no calibration shift was applied.

The ν_9 spectra were less straightforward as the band is very weak. The previous normal propane ν_9 spectra[6] used 3 Torr pressure in a cell with twice the path length, and intensity measurements by Kondo and Saëki[34] imply the ν_9 band strength is 10-20 times weaker than ν_{26}. We were thus limited by the amount of sample available to us; the White cell has a volume of approximately 300 litres so 1 gram of sample gives rise to only 1 Torr pressure in the cell. We ended up using all of the available sample, giving 3.040 Torr pressure at 296 ± 1K, and recorded a spectrum at this temperature (191 scans) and a cooled spectrum at 217.25K (224 scans). The cooling lowered the pressure to 2.225 Torr. A 6 μm Mylar beam splitter was used in this region along with an entrance aperture of 1.5 mm. Water lines in the room temperature spectra were used to check the calibration of the spectrum against values from HITRAN[41], and no adjustment was required. The low-temperature spectrum froze out the otherwise rather strong absorptions from residual water in the cell making propane measurements easier. It also reduced the hot band intensity somewhat and made their identification clearer. The room temperature spectrum was used to extend the assignments to higher *J* and *K* values. The spectra are included in the supplementary data[47] deposited in the University of Bristol data repository.

Results and Analysis

A survey scan of the bands around ν_{26} is shown in Figure 1. It was not possible to completely eliminate 2-^{13}C-propene from the sample, and several bands from this species were visible in our spectra, specifically ν_{20} (A"), ν_{19} (A") and ν_{18} (A"). The figure also includes a spectrum of moderate resolution of normal propane for comparison, demonstrating some obvious isotopic shifts caused by the ^{13}C substitution. The band origins can offer valuable information for force field calculation refinements and so we include Table 1 a list of these for the bands observed in this study. Where high-resolution analyses have been done we use those values; for the other bands we have estimated band origins. Values for normal propane are included for reference.

Table 1 Origins (/cm^{-1}) of selected vibrational bands of propane

Band	Normal Propane	2-^{13}C-Propane[a]	Shift
ν_9 (A_1)	369.222 808(25)[b]	366.766 695 1(74)	-2.456 113
ν_{26} (B_2)	748.530 882(80)[c]	746.614 150 7(80)	-1.916 731
ν_8 (A_1)	870.39575(160)[d]	863	-7
ν_{21} (B_1)	921.3756(400)[d]	920.85	-0.53
ν_{20} (B_1)	1054.2[e]	1039.5	-14.7
ν_7 (A_1)	1157[e]	1148	-9
ν_{25} (B_2)	1192[e]	1182	-10

[a] This work
[b] Ref [6]
[c] Ref [5]
[d] Ref [9]
[e] From the PNNL database [48] as available from HITRAN [49].

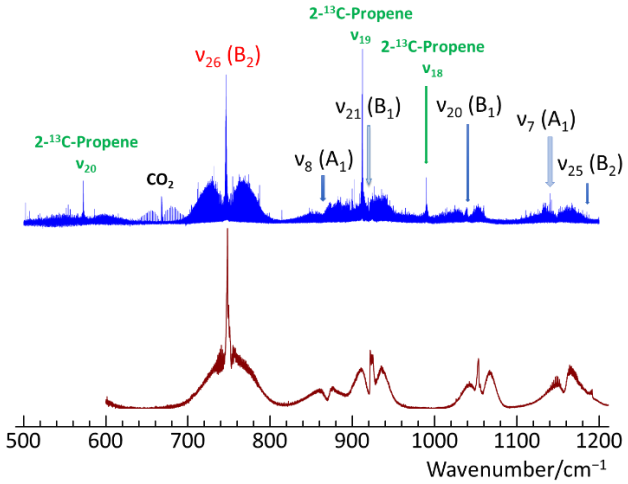

Figure 1. Survey scan (upper trace) of our 2-^{13}C-Propane sample at 0.065 Torr. The 2-^{13}C-Propane bands are labelled according to the conventions used in previous work[5, 6, 8, 50]. The 2-^{13}C-Propene impurity peaks are labelled in green. The lower trace is a low-resolution spectrum of normal propane for comparison, taken from PNNL[48] as available from the HITRAN database[49].

Initial Analysis of the ν_{26} Region

An overview of the ν_{26} region is shown in Figure 2. An initial simulation for ν_{26} was set up using the ground state constants from Lide[36], and taking the vibrational changes in those constants from the normal propane study of ν_{26} [5]. The result is similar at first glance to the c-type band seen in normal propane. The analysis was

started before the automated assignment tools[51] in PGOPHER were available, so a traditional approach to assignment was used based on picking out related branches. In this case the $^{r}R_{Ka}(J)$ and $^{p}P_{Ka}(J)$ branches (for a given K_a) can be tracked back to their matching $^{r}Q_{Ka}$ and $^{p}Q_{Ka}$ band heads, paying attention to the "missing" lines for each particular K_a subband value, as shown in Figure 3. The Q-branch heads were assigned readily by comparing them to the normal propane spectrum and by their approximate distances from the front of the central Q-branch head near 746.42 cm^{-1}. The correctness of the $^{p}Q_{Ka}$ and $^{r}Q_{Ka}$ assignments could then be verified by the "missing lines" in a particular K_a series of J lines as they were tracked back to their subband origins near the front of each Q branch head. Tentative assignments of the $^{r}R_{Ka}(J)$ and $^{p}P_{Ka}(J)$ lines could then be made in PGOPHER, and then fitted to upper state rotational constants initially, and then centrifugal distortion constants and lower state constants as the fit progressed. This simple process could be continued for K_a' values up to 14, giving the preliminary fit presented at the 2017 ISMS[45], with some 3500 lines and an average residual of about 2 x 10^{-4} cm^{-1}. At this stage the residuals (Figure 4) were showing a systematic trend at higher K_a' values, and there was some evidence of "extra" lines appearing among the ^{r}R and ^{p}P lines out in the wings of the band. This implies the perturbation seen in the normal propane is also visible here, requiring information on ν_9 and $2\nu_9$, which is best obtained from the ν_9 region.

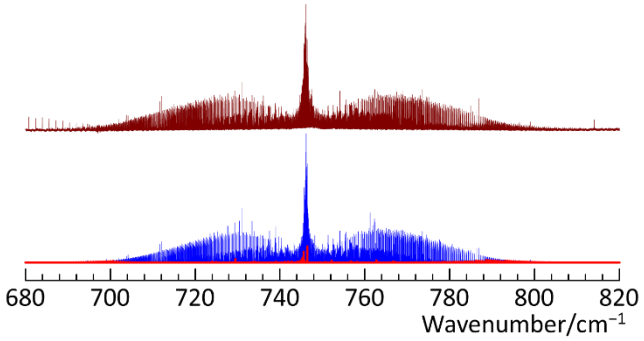

Figure 2. Overview of the region of the $\nu_{26}(B_2)$ c-type band in 2-^{13}C-propane. The top trace is the experimental spectrum, and the lower trace is the PGOPHER simulation using the constants in Table 2 and Table 3, with the ν_{26} lines in blue and the perturbation-allowed transitions in red. The left edge of the observed spectrum includes some CO_2 lines that were used for calibration.

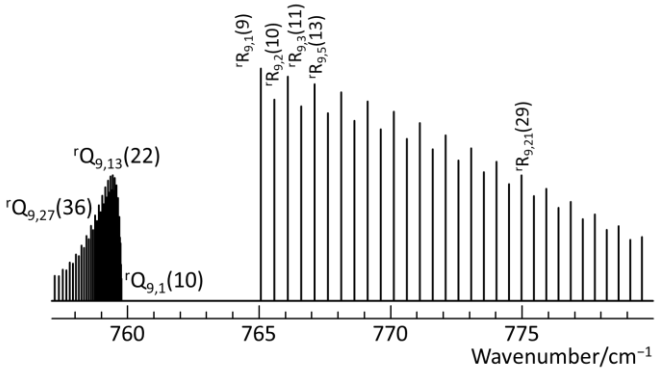

Figure 3. Typical ^{r}Q band head and linked ^{r}R branch used in initial assignment. This is for K_a'' = 9, but a very similar pattern is seen for other K_a, but with the gap between the ^{r}Q band head and the first ^{r}R branch line increasing with K_a. Lines calculated with PGOPHER.

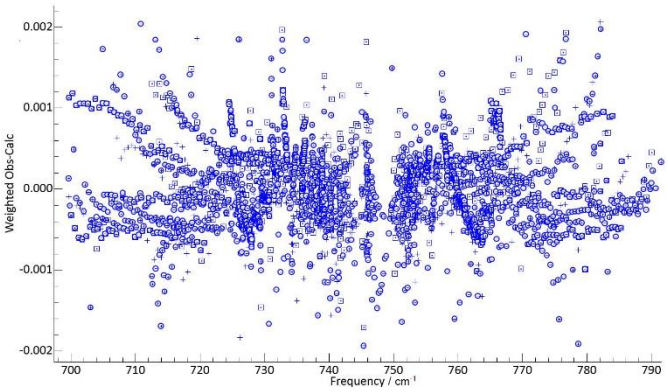

Figure 4 Residuals from the initial fit[45] to the ν_{26} band of 2-^{13}C-propane showing the effect of the perturbation caused by the a-type Coriolis interaction with $2\nu_9$ levels

Analysis of the ν_9 Region

The ν_9 band has the classic asymmetric rotor b-type band appearance with strong P and R branches and a central gap (Figure 5), just as in normal propane. The ν_{14} (A') CCC bending band of 2-^{13}C-propene shows strongly at the high frequency side of this spectrum, but fortunately the very high-resolution of the CLS interferometer made it easy to differentiate the lines of the two species. A preliminary analysis of the ν_{14} band of 2-^{13}C-propene was presented at the 2017 ISMS meeting [52], and a full analysis of this and the ν_{14} band of normal propene is in progress.

An initial simulation was set up as for the ν_{26} band of 2-^{13}C-propane, using the changes in rotational constants from normal propane[6]. The first useful feature for assignment was the clear $^{r}Q_0(J)$ lines from 367.4 – 368.5 cm^{-1} (Figure 6). This allowed the $^{p}Q_{Ka}$ and $^{r}Q_{Ka}$ band heads to be easily assigned, and then the fit extended to the entire band, walking up in J and K. For ν_9 we used PGOPHER to plot out some Loomis-Wood diagrams to check some of the branches since this band was denser in line distribution. There were also many secondary band heads caused by lines in some Q branches turning back on themselves especially at the lower K_a values. The ν_9 band proved to be unperturbed, as in normal propane, and the fit could be extended to the entire band, giving values for upper and lower state rotational constants and centrifugal distortion constants to 4th order.

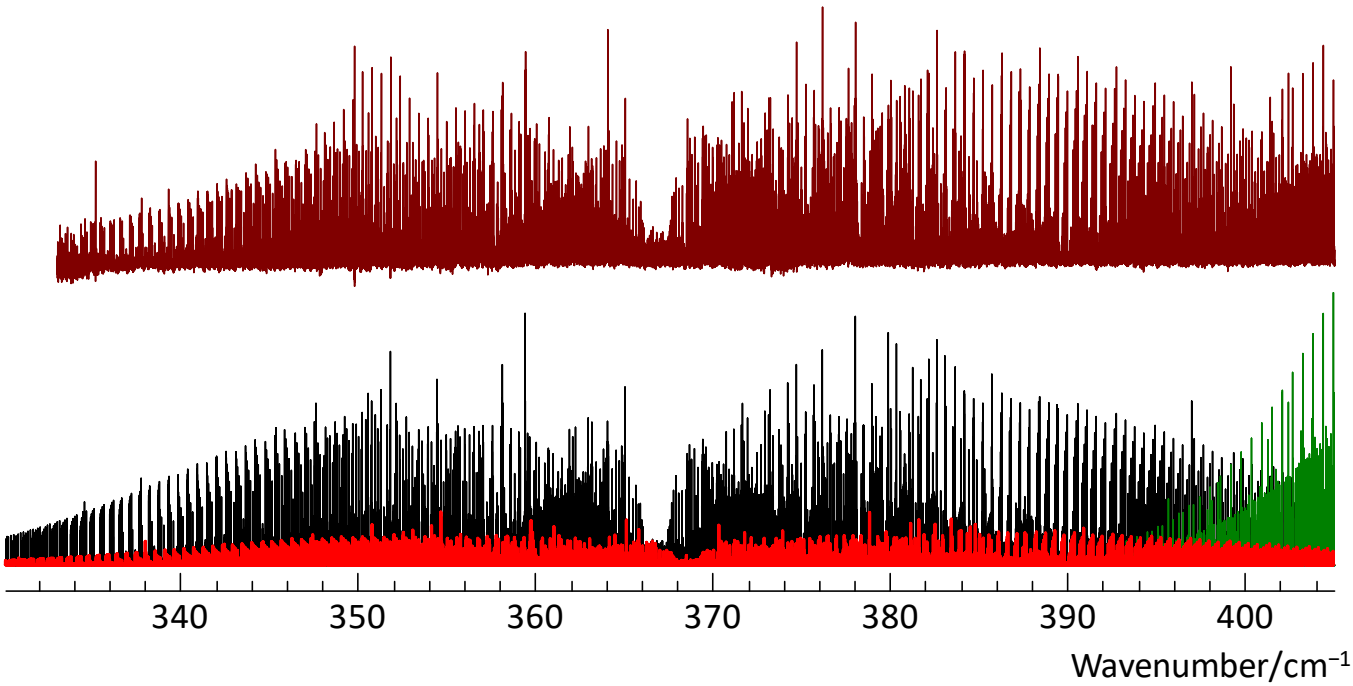

Figure 5 Overview of the region of the ν_9 (A_1) b-type band in 2-^{13}C-propane. The top trace is the experimental spectrum, and the lower trace is the PGOPHER simulation using the constants in Table 2 and Table 3.The colors in the simulation are black for ν_9, red for $2\nu_9$-ν_9 and the green lines are for the ν_{14}(A_1) band of 2-^{13}C-propene.

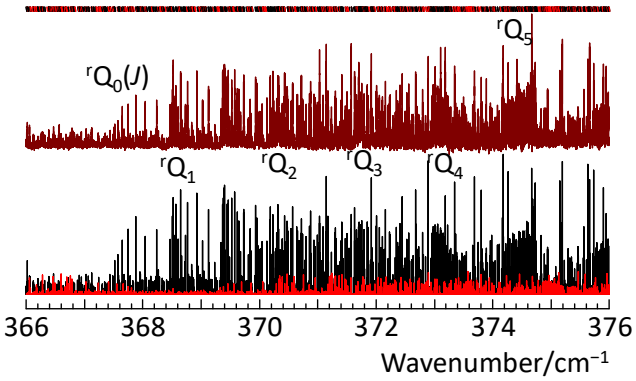

Figure 6 Close up of the ν_9(A_1) band center at 366.7667 cm^{-1} of 2-^{13}C-propane. See Figure 5 caption for color information. Tick marks at the top indicate lines included in the fit.

Close inspection of the spectrum revealed, as in normal propane, many weaker lines from hot bands. A clear pattern is seen of Q branch heads from the $2\nu_9$–ν_9 hot bands, particularly on the P-side (Figure 7). Comparison of the room temperature and cooled spectra confirmed the assignment to hot bands. The specific assignment to ν_9 = 1 as the lower state was confirmed via combination differences. A number of assignments were then possible from this spectrum, but as expected systematic errors became visible as the range of K_a' was increased. This confirmed the necessity for a combined fit to all the interacting states simultaneously.

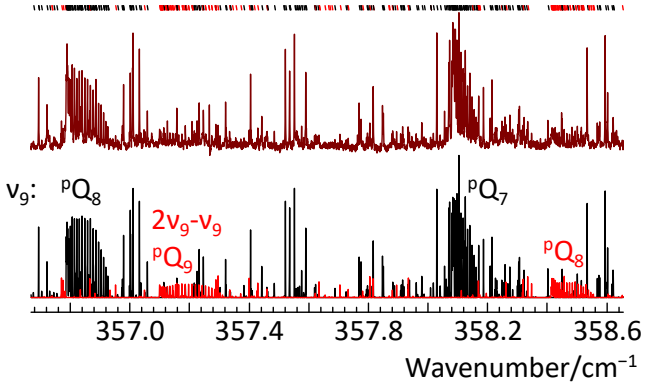

Figure 7 Expanded plot of the ν_9(A_1) band of 2-^{13}C-propane showing the $2\nu_9$-ν_9 hot band Q branches ($^pQ_9$ and $^pQ_8$) in red. See also the Figure 6 caption.

Combined fit to all states

To model the interaction between ν_{26} and $2\nu_9$ we added an a-type Coriolis resonance, as was done for the ν_{26} band of normal propane[5]. This was done using the general purpose perturbation mechanism built into PGOPHER[44]; the earlier analysis was done with a program written by JMF but the underlying calculation methods and matrix elements are essentially identical and the constants from [5] will simulate the normal propane spectrum in PGOPHER. The first order Coriolis mixing term, $\langle v26=1|\hat{J}_a|v9=2\rangle$, clearly improved the fits for both ν_{26} and $2\nu_9$ and a straight forward trial and error process accompanied by re-fitting could then be used to assign all the remaining lines from ν_{26} and $2\nu_9$ in our spectra. The fitting process at this stage used was a simultaneous fit to all states, which predicted some perturbation-allowed $2\nu_9 \leftarrow 0$ transitions. (It was clear from

the initial analysis that this overtone transition is otherwise too weak to see under the conditions we used.) The perturbation-allowed transitions are strong for many lines with K_a' between 18 and 26, with an additional smaller cluster with K_a' = 1 – 5. The large cluster at higher K_a' arises because the separation between ν_{26} and $2\nu_9$ is essentially J independent for K_a' > 10, and near degenerate for K_a' = 23 and 24, with the order swapping over, as shown in Figure 8(a). The cluster at lower K_a' arises because of the different pattern of levels for low K_a' for an asymmetric top, giving a few localized crossings, as shown in Figure 8(b). Both clusters gave lines strong enough to include in our fit, adding 543 lines in total, with 520 from the high K_a' cluster. This is to be compared with 8689 from ν_{26}. See Figure 9 for a small sample section of the ν_{26} spectrum showing the strength and number of $2\nu_9$ lines present.

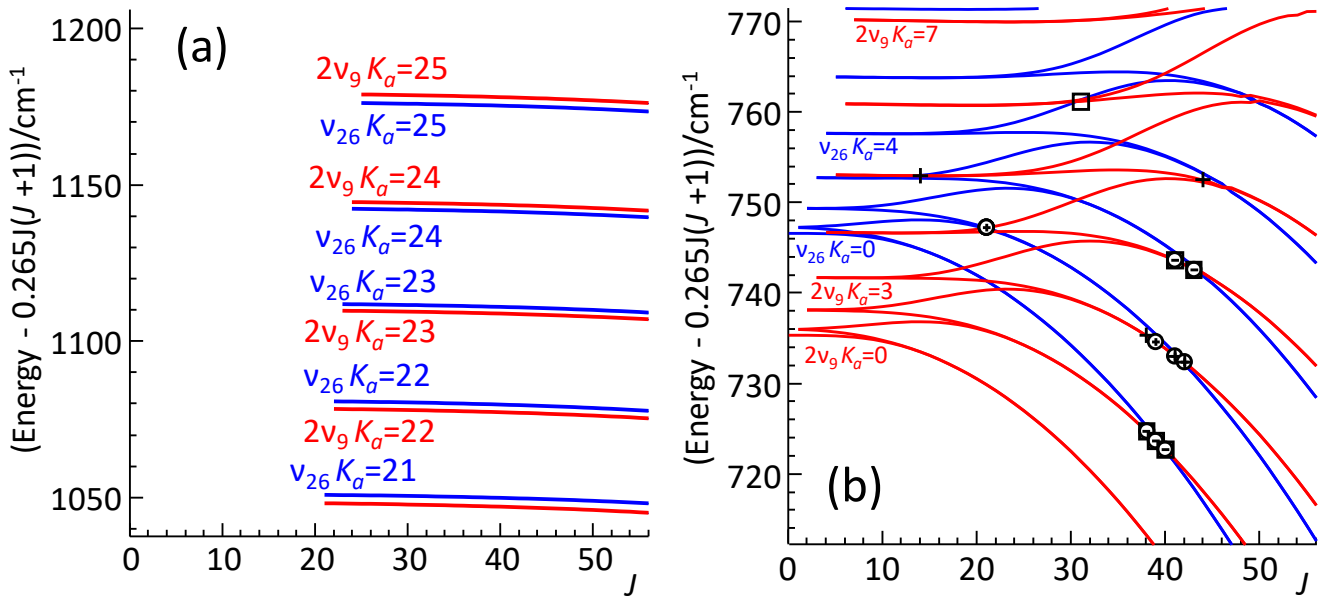

Figure 8 Reduced energy level plot for plot of selected energy levels of ν_{26} and $2\nu_9$ showing (a) the large scale interaction around K_a = 23 and 24, giving perturbation-allowed transitions to all the $2\nu_9$ levels in the diagram and (b) the localized crossings at low K_a affecting only a few levels. The symbols in (b) indicate levels involved in perturbation-allowed transitions included in the final fit.

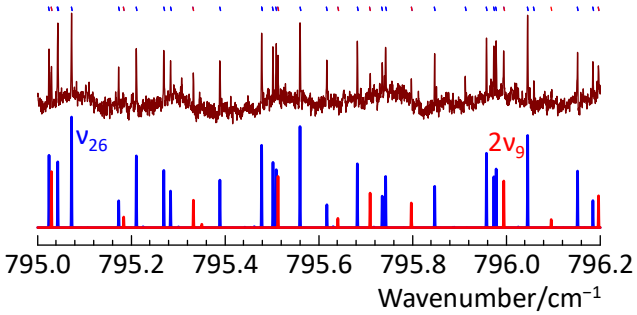

Figure 9 Section of the R-side of the ν_{26} band where the perturbation-allowed transitions are significant. Colors as in Figure 2; the tick marks at the top indicate lines included in the fit.

In completing our line list we also found an additional small local perturbation in ν_{26} around K_a' = 9. The shifts introduced by this state are typically small (< 0.004 cm^{-1}) but are clear in our analysis. We can model this perturbation by introducing a state of B_1 symmetry which we call P and adding a b-type Coriolis interaction between this and ν_{26}. One perturbation-allowed transition is visible to this state, but most of the information on it comes from the displacement of the ν_{26} levels so we were only able to determine a relatively limited

amount about this state, and we cannot rule out alternative interpretations of this perturbation. This state must involve some combination of the ν_{14} or ν_{27} torsional levels but with sufficient torsional quanta involved that it is not possible to develop a more quantitative model at the present time. The parameters for this P state must be regarded as effective parameters, but they are sufficient to bring the residuals for the perturbed transitions into line with the rest of the fit, and the effect on intensities is small. Apart from the Coriolis mixing terms described here, the Hamiltonian is the standard Watson A reduced form[53] in the I^r representation.

Our final list had 20185 assigned lines covering the ν_9, ν_{26} and $2\nu_9$-ν_9 bands. To determine ground state constants we used this line list to generate 10625 ground state combination differences from 18309 of the observations; 1876 of the full set did not involve a combination difference and were not included in the fit. The final constants are listed in Table 2, including values from the microwave study by Lide[36] and the *ab initio* predictions[39], indicating good agreement with both. Details of the fit, including observed – calculated values for each line and the matrix elements used are available in the supplementary data[47]. Because of the high precision of the low order rotational constants from our fit, the ground state constants reproduce the microwave lines (which have $J \leq 7$¸ $K_a \leq 1$) to an average error of 33 kHz, easily within the estimated 66 kHz error of the measurements. These are not included in the final ground state fit, as they do not significantly change any of the constants.

Table 2 Rotational constants (/cm^{-1}) for the ground vibrational state of 2-^{13}C-propane.

	This work	Microwave[b]	*Ab initio*[c]
A	0.956 017 58(19)	0.956 011 4(33)	0.955 135
B	0.281 755 72(11)	0.281 765 3(33)	0.281 893
C	0.247 608 69(11)	0.247 611 0(33)	0.247 578
Δ_K	5.373 61(39) x 10^{-6}		5.580 x 10^{-6}
Δ_{JK}	-9.025 4(29) x 10^{-7}		-10.21 x 10^{-7}
Δ_J	2.377 27(81) x 10^{-7}		2.475 x 10^{-7}
δ_K	1.131(16) x 10^{-7}		1.392 x 10^{-7}
δ_J	4.774 0(36) x 10^{-8}		5.960 x 10^{-8}
Φ_K	1.151(18) x 10^{-10}		
Φ_{KJ}	-4.329(262) x 10^{-11}		
Φ_{JK}	1.71(79) x 10^{-12}		
Φ_J	2.69(23) x 10^{-13}		
ϕ_K	3.3(22) x 10^{-11}		
ϕ_{JK}	2.52(84) x 10-12		
ϕ_J	1.15(12) x 10-13		
σ	0.000 12	3.3 x 10^{-6}	
n_{obs}	10 625[a]	6	

[a] The ground state constants were determined by fitting to ground state combination differences computed from 18309 of the observations; 1876 of the full set did not involve a combination difference and were not used in the fit.

[b] Reference [36]; only 6 $K_a = 1 \leftarrow 0$ lines were observed.

[C] Reference [39].

The final constants for all the other states were derived from a simultaneous fit to the constants for all the other states, keeping the ground state constants fixed at the values from the combination difference fit. Our

line list necessarily included a significant number of blends given the line density; these were handled with the standard approach of combining blended lines into a single effective observation, weighted by the calculated relative intensity of the lines. For the excited state fit this reduced 20185 to 14296 effective observations. The constants are given in Table 3, and the average error of this all band fit was 0.00016 cm^{-1}, about 10% of the linewidth of 0.00096 cm^{-1}, and showing no sign of systematic trends in the residuals – see Figure 10. Details of the fit, including observed – calculated values for each line and the matrix elements used are available in the supplementary data[47]. Also included is an alternative fit to the same line list, allowing the ground state constants to float also; this only causes minor changes to the constants, so the separate fits are recommended. The fit is reasonably similar to the values for normal propane; the main Coriolis matrix element is 0.0425 as compared to 0.0446 for normal propane[5] and only one additional Coriolis parameter was required here as compared to 3 for normal propane, but this difference is probably not significant.

The quality of the fit can be seen from Figure 10 and selected regions of the spectrum shown in Figure 11; see also the other figures including spectra in the paper, all of which include simulated spectra using the final constants along with the experimental spectra. There are a significant number of weaker lines in the spectra that we do not assign, but this is to be expected as hot bands involving the torsional modes are to be expected. Indeed given that the hot band involving v_9 at 366 cm^{-1} figures so prominently in our analysis, it is perhaps surprising that the low frequency torsion levels at 217 cm^{-1} and 265 cm^{-1} [42] are not stronger, but they are visible as rather congested spectra under the assigned lines.

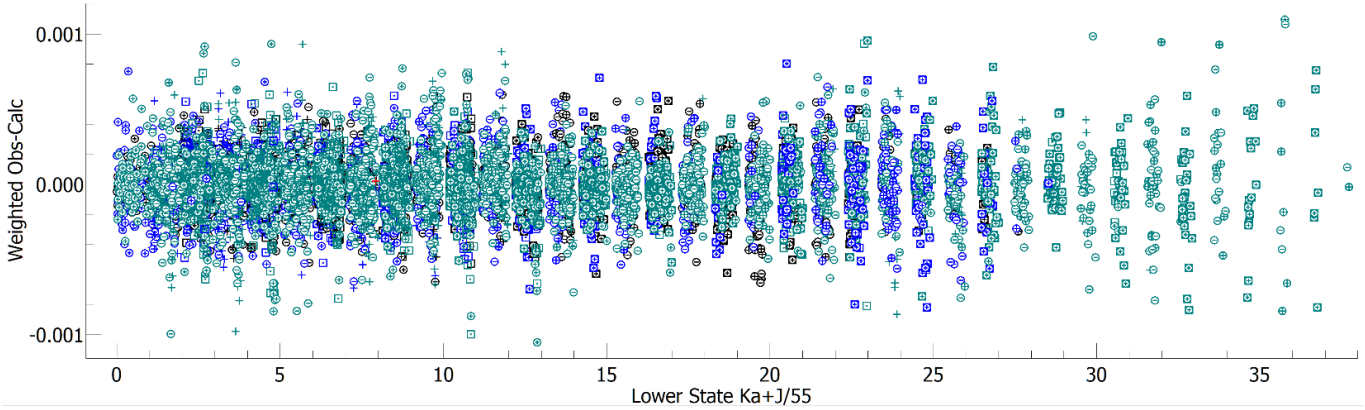

Figure 10 Residuals for the combined fit to v_{26} (shown in Teal), $2v_9$ (blue) and v_9 (black, mostly hidden under the other states).

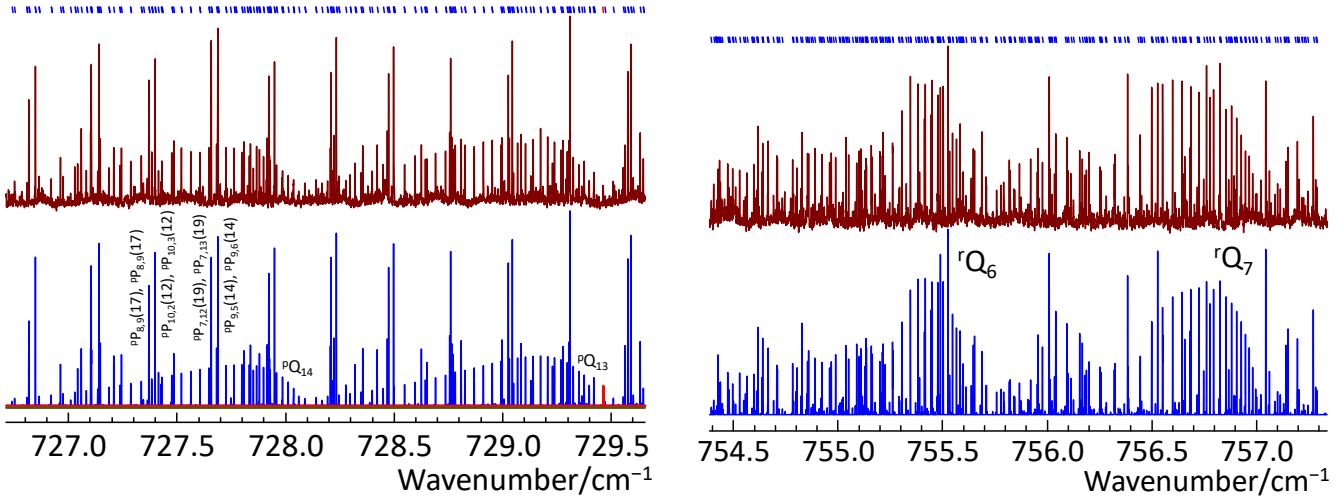

Figure 11 Simulations of selected regions of the ν_{26} band. Colors as in Figure 2; the tick marks at the top indicate lines included in the fit.

Table 3 Rotational constants for the v_9, $2v_9$ and v_{26} vibrational states of 2-^{13}C-propane.

Constants / cm^{-1}	**v_9 = 1**	**v_9 = 2**	**v_{26} = 1**	**P**[a]
v_0	366.766 695 1(74)	735.331 880 2(99)	746.614 1507(80)	759.438 45(774)
A	0.966 838 13(13)	0.977 747 76(18)	0.956 326 69(13)	0.939 883(92)
B	0.281 560 898(57)	0.281 357 930(47)	0.280 916 552(37)	0.280 893 96(845)
C	0.246 955 160(55)	0.246 303 861(43)	0.246 906 812(38)	0.244 903 93(832)
Δ_K	6.088 74(46) x 10^{-6}	6.878 25(61) x 10^{-6}	5.404 177(486) x 10^{-6}	c
Δ_{JK}	-8.682 7(22) x 10^{-7}	-8.329 8(19) x 10^{-7}	-8.864 22(230) x 10^{-7}	c
Δ_J	2.329 149(370) x 10^{-7}	2.268 10(16) x 10^{-7}	2.363 633(273) x 10^{-7}	3.435 7(187) x 10^{-7}
δ_K	2.125(19) x 10^{-7}	2.811 8(83) x 10^{-7}	1.215 1(41) x 10^{-7}	c
δ_J	4.691 2(31) x 10^{-8}	4.542 2(12) x 10^{-8}	4.774 34(73) x 10^{-8}	c
Φ_K	2.099 7(218) x 10^{-10}	2.772 7(66) x 10^{-10}	1.174 5(197) x 10^{-10}	c
Φ_{KJ}	-5.405(305) x 10^{-11}	-4.847(31) x 10^{-11}	-4.768 2(2677) x 10^{-11}	c
Φ_{JK}	4.167(914) x 10^{-12}	0	2.434 6(8028) x 10^{-12}	c
Φ_J	2.690(145) x 10^{-13}	0	1.385(70) x 10^{-13}	c
φ_K	1.043(252) x 10^{-10}	0	6.71(215) x 10^{-11}	c
φ_{JK}	5.24(92) x 10^{-12}	0	0	c
φ_J	1.212(97) x 10^{-13}	0	0	c
L_K	0	0	-2.459(240) x 10^{-15}	0
L_{KKJ}	0	0	3.779(205) x 10^{-15}	0
L_{JK}	0	0	-2.129(114) x 10^{-15}	0
L_{JJK}	0	0	2.069(400) x 10^{-16}	0
$\langle v26=1\|\hat{J}_a\|v9=2\rangle$		0.0424 901 9(80)		
$\langle v26=1\|\hat{J}_a\hat{J}^2\|v9=2\rangle$		1.012 79(51) x 10^{-6}		
$\langle P\|\hat{J}_b\|v26=1\rangle$			6.20(15) x 10^{-4}	
$\langle P\|\hat{J}_b\hat{J}^2\|v26=1\rangle$			9.734(78) x 10^{-7}	
σ	0.000 16			
n	14 296[b]			

a. The identity of this state is unknown, but must involve one or both torsional modes

b. There were 20185 observations before combining blends

c. Constrained to the ground state values in Table 2

Conclusions

The fitting of the ground, ν_9, $2\nu_9$ and ν_{26} vibrational states of 2-^{13}C-propane has yielded molecular constants taking into account perturbations of sufficient quality to reproduce the observed ν_9, $2\nu_9$-ν_9 and ν_{26} bands to 0.00016 cm^{-1}. This will provide the position part of a linelist but, while the model presented here gives good relative intensities, absolute intensities will require a good model for the torsional vibrations to allow a complete partition function calculation. This has been discussed by Perrin et al [9] for normal propane.

The bands we have analyzed here are not affected by the torsional motions; the torsional splittings are probably comparable to the ground state torsional splittings of only a few MHz[54], so would require much higher resolution to be visible. However the ν_8 and ν_{21} bands in normal propane show strong interactions with torsional motions and the analysis of these bands in normal propane required a model including states with two quanta in the torsional modes [9], and these bands are also visible in our spectra, and an analysis of these bands is likely to be the most informative about the torsion modes.

The methodology used here can be extended in a straightforward way to other isotopologues; preliminary results for 2,2-D_2-[55, 56], 1-^{13}C-[57], 2-D_1- [58] and 1-D_1- [59] substituted propanes have been presented, and we also have preliminary analyses for the CCC bending modes of the 1,1,1-D_3-, 1,1,1,3,3,3-D_6- and D_8- propane species [ν_{16}(A'), ν_9(A_1) and ν_9(A_1), respectively]. There are no experimentally determined values of rotational constants reported for these molecules in the literature. Analyses of these species are sped up significantly by using the nearest lines functionality recently added to PGOPHER, which allows rapid expansion of an initial assignment to cover an entire band, and these results will be described in follow up publications.

Acknowledgements

Firstly, SJD wants to note that this project was only made possible by Jon Hougen, who organized our collaboration in the first place and then set up our meetings at NIST with WJL and JMF. He also arranged the initial collaboration with BB at the 2014 ISMS meeting. He kept encouraging SJD at every subsequent meeting thereafter in this project until his untimely passing.

Dr. Bob McKellar (NRCC) made the initial suggestion at ISMS 2014 to work on the isotopologues when SJD was told by Olivier Pirali (SOLEIL-Ailes) that JMF and WFL had recently finished a re-analysis of the ν_{26} band of normal propane.

John Kilby of ICON Isotopes made extra efforts to locate for SJD a collaborator at Berry & Associates to perform the synthesis of the 2-^{13}C-Propane.

Dennis Tokaryk and Scott Goudreau (University of New Brunswick) helped SJD in the early stages of this work with how to use the PGOPHER program.

SJD also thanks the University of Tennessee Knoxville for its support through continued access to library and computer facilities after retirement from teaching and advising duties. He also wants to thank the Department of Physics & Astronomy of UTK, especially Professor Hanno Weitering, for his support of this project and for providing funds to purchase the sample of 2-^{13}C-Propane.

The authors would like to thank Dr. Iouli Gordon at the Harvard-Smithsonian Center for Astrophysics for his help with the HITRAN listings we needed for checking calibration.

The spectra described in this paper were obtained at the Canadian Light Source, which is supported by the Canada Foundation for Innovation, Natural Sciences and Engineering Research Council of Canada, the University of Saskatchewan, the Government of Saskatchewan, Western Economic Diversification Canada, the National Research Council Canada, and the Canadian Institutes of Health Research

References

[1] Maguire WC, Hanel RA, Jennings DE, Kunde VG, Samuelson RE. C_3H_8 and C_3H_4 in Titan's atmosphere. Nature. 1981;292:683-6. 10.1038/292683a0

[2] Atakan AA, Blass WE, Brault JW, Daunt SJ, Halsey GW, Jennings DE, et al. The 13.37 Micron Band of Propane: A Spectral Catalog from 700 cm^{-1} to 800 cm^{-1}. Dept. of Physics & Astronomy, Univ. of Tennessee; 1988.

[3] Nixon CA, Jennings DE, Flaud JM, Bézard B, Teanby NA, Irwin PGJ, et al. Titan's prolific propane: The Cassini CIRS perspective. Planetary and Space Science. 2009;57:1573-85. 10.1016/j.pss.2009.06.021

[4] Roe HG, Greathouse TK, Richter MJ, Lacy JH. Propane on Titan. The Astrophysical Journal. 2003;597:L65-L8. 10.1086/379816

[5] Flaud JM, Kwabia Tchana F, Lafferty WJ, Nixon CA. High resolution analysis of the ν_{26} and $2\nu_9$–ν_9 bands of propane: modelling of Titan's infrared spectrum at 13.4 µm. Mol Phys. 2010;108:699-704. 10.1080/00268970903501709

[6] Kwabia Tchana F, Flaud JM, Lafferty WJ, Manceron L, Roy P. The first high-resolution analysis of the low-lying ν9 band of propane. Journal of Quantitative Spectroscopy and Radiative Transfer. 2010;111:1277-81. 10.1016/j.jqsrt.2009.12.009

[7] Flaud JM, Lafferty WJ, Herman M. First high resolution analysis of the absorption spectrum of propane in the 6.7 µm to 7.5 µm spectral region. The Journal of Chemical Physics. 2001;114:9361-6. 10.1063/1.1368386

[8] Perrin A, Kwabia-Tchana F, Flaud JM, Manceron L, Demaison J, Vogt N, et al. First high resolution analysis of the ν_{21} band of propane $CH_3CH_2CH_3$ at 921.382cm^{-1}: Evidence of large amplitude tunneling effects. J Mol Spectrosc. 2015;315:55-62. 10.1016/j.jms.2015.02.010

[9] Perrin A, Flaud JM, Kwabia-Tchana F, Manceron L, Groner P. Investigation of the ν_8 and ν_{21} bands of propane $CH_3CH_2CH_3$ at 11.5 and 10.9 µm: evidence of large amplitude tunnelling effects. Mol Phys. 2019;117:323-39. 10.1080/00268976.2018.1512720

[10] Niemann HB, Atreya SK, Carignan GR, Donahue TM, Haberman JA, Harpold DN, et al. Chemical composition measurements of the atmosphere of Jupiter with the Galileo Probe mass spectrometer. Advances in Space Research. 1998;21:1455-61. https://doi.org/10.1016/S0273-1177(98)00019-2

[11] Greathouse TK, Lacy JH, Bézard B, Moses JI, Richter MJ, Knez C. The first detection of propane on Saturn. Icarus. 2006;181:266-71. https://doi.org/10.1016/j.icarus.2005.09.016

[12] Guerlet S, Fouchet T, Bézard B, Simon-Miller AA, Michael Flasar F. Vertical and meridional distribution of ethane, acetylene and propane in Saturn's stratosphere from CIRS/Cassini limb observations. Icarus. 2009;203:214-32. https://doi.org/10.1016/j.icarus.2009.04.002

[13] Moses JI, Bézard B, Lellouch E, Gladstone GR, Feuchtgruber H, Allen M. Photochemistry of Saturn's Atmosphere: I. Hydrocarbon Chemistry and Comparisons with ISO Observations. Icarus. 2000;143:244-98. https://doi.org/10.1006/icar.1999.6270

[14] Beale CA, Hargreaves RJ, Bernath PF. Temperature-dependent high resolution absorption cross sections of propane. Journal of Quantitative Spectroscopy and Radiative Transfer. 2016;182:219-24. 10.1016/j.jqsrt.2016.06.006

[15] Wong A, Appadoo DRT, Bernath PF. IR absorption cross sections of propane broadened by H_2 and He between 150 K and 210 K. Journal of Quantitative Spectroscopy and Radiative Transfer. 2018;218:68-71. 10.1016/j.jqsrt.2018.06.026

[16] Sung K, Toon GC, Mantz AW, Smith MAH. FT-IR measurements of cold C_3H_8 cross sections at 7–15µm for Titan atmosphere. Icarus. 2013;226:1499-513. https://doi.org/10.1016/j.icarus.2013.07.028

[17] Kleiner I. Spectroscopy of Interstellar Internal Rotors: An Important Tool for Investigating Interstellar Chemistry. ACS Earth and Space Chemistry. 2019;3:1812-42. 10.1021/acsearthspacechem.9b00079

[18] Li B, Ho SSH, Gong S, Ni J, Li H, Han L, et al. Characterization of VOCs and their related atmospheric processes in a central Chinese city during severe ozone pollution periods. Atmos Chem Phys. 2019;19:617-38. 10.5194/acp-19-617-2019
[19] Paoletti E, De Marco A, Beddows DCS, Harrison RM, Manning WJ. Ozone levels in European and USA cities are increasing more than at rural sites, while peak values are decreasing. Environmental Pollution. 2014;192:295-9. https://doi.org/10.1016/j.envpol.2014.04.040
[20] Sherwood Lollar B, Westgate TD, Ward JA, Slater GF, Lacrampe-Couloume G. Abiogenic formation of alkanes in the Earth's crust as a minor source for global hydrocarbon reservoirs. Nature. 2002;416:522-4. 10.1038/416522a
[21] Burruss RC, Laughrey CD. Carbon and hydrogen isotopic reversals in deep basin gas: Evidence for limits to the stability of hydrocarbons. Organic Geochemistry. 2010;41:1285-96. 10.1016/j.orggeochem.2010.09.008
[22] Laughrey CD, Baldassare FJ. Applications of Stable Isotope Geochemistry in the Petroleum Geosciences. Petroleum Technology Transfer Council (PTTC); 2014.
[23] McMurry HL, Thornton V, Condon FE. Infra-Red Spectra of Propane, 1-Deuteropropane, and 2-Deuteropropane and Some Revisions in the Vibrational Assignments for Propane. The Journal of Chemical Physics. 1949;17:918-22. 10.1063/1.1747087
[24] McMurry HL, Thornton V. The Infra-Red Spectra of Propane and 2,2-Dideuteropropane. Journal of Chemical Physics. 1950;18:1515-6. 10.1063/1.1747529
[25] McMurry HL, Thornton V. The Infrared Spectra of Propane and Its Symmetrical Deuterium Substituted Analogs. Journal of Chemical Physics. 1951;19:1014-8. 10.1063/1.1748443
[26] McMurry HL, Speas D. Vibrational analysis of propane and its symmetrical deuterium substituted isomers. Spectrochimica Acta. 1965;21:2105-17. 10.1016/0371-1951(65)80226-0
[27] Friedman L, Turkevich J. The Infra-Red Absorption Spectra of Propane-D−1 and Propane-D−2. The Journal of Chemical Physics. 1949;17:1012-5. 10.1063/1.1747105
[28] Gayles JN, King WT. The infrared spectrum of propane. Spectrochimica Acta. 1965;21:543-57. 10.1016/0371-1951(65)80145-X
[29] Gayles JN, King WT, Schachtschneider JH. Quadratic potential constants for propane. Spectrochimica Acta Part A: Molecular Spectroscopy. 1967;23:703-15. 10.1016/0584-8539(67)80324-6
[30] Pearce RAR, Levin IW. Normal coordinate treatment for propane: Force constant selection through a backward elimination regression–refinement procedure. Journal of Chemical Physics. 1979;70:370-9. 10.1063/1.437199
[31] Gough KM, Baudais FL, Casal HL. Vibrational analysis of $CD_3CD_2CD_3$, CD_3CHDCD_3, and $CHD_2CD_2CD_3$ in the 100 – 11500 cm^{-1} spectral range. Journal of Chemical Physics. 1986;84:549-60. 10.1063/1.450601
[32] Gough KM, Murphy WF, Raghavachari K. The harmonic force field of propane. The Journal of Chemical Physics. 1987;87:3332-40. 10.1063/1.453027
[33] Gough KM, Murphy WF, Stroyer-Hansen T, Svendsen ENr. Raman trace scattering intensity parameters for propane. The Journal of Chemical Physics. 1987;87:3341-6. 10.1063/1.453028
[34] Kondo S, Saëki S. Infrared absorption intensities of ethane and propane. Spectrochimica Acta Part A: Molecular Spectroscopy. 1973;29:735-51. 10.1016/0584-8539(73)80103-5
[35] Loh A, Wolff M. Absorption cross sections of ^{13}C ethane and propane isotopologues in the 3µm region. Journal of Quantitative Spectroscopy and Radiative Transfer. 2017;203:517-21. 10.1016/j.jqsrt.2017.05.012
[36] Lide Jr. DR. Microwave Spectrum, Structure, and Dipole Moment of Propane. Journal of Chemical Physics. 1960;33:1514-8. 10.1063/1.1731434
[37] Blom CE, Altona C. Application of self-consistent-field ab initio calculations to organic molecules. Mol Phys. 1976;31:1377-91. 10.1080/00268977600101081
[38] Fischer P, Grunenberg A, Bougeard D, Schrader B. Coupled calculation of vibrational frequencies and intensities: Part IX. Intensities of methane, ethane, propane, and methionine calculated with the MNDO method. Journal of Molecular Structure. 1986;146:51-60. https://doi.org/10.1016/0022-2860(86)80281-2
[39] Villa M, Senent ML, Carvajal M. Highly correlated ab initio study of the low frequency modes of propane and various monosubstituted isotopologues containing D and ^{13}C. Physical chemistry chemical physics : PCCP. 2013;15:10258-69. 10.1039/c3cp50213a
[40] Jacquinet-Husson N, Armante R, Scott NA, Chédin A, Crépeau L, Boutammine C, et al. The 2015 edition of the GEISA spectroscopic database. J Mol Spectrosc. 2016;327:31-72. https://doi.org/10.1016/j.jms.2016.06.007

[41] Gordon IE, Rothman LS, Hill C, Kochanov RV, Tan Y, Bernath PF, et al. The HITRAN2016 molecular spectroscopic database. Journal of Quantitative Spectroscopy and Radiative Transfer. 2017;203:3-69. https://doi.org/10.1016/j.jqsrt.2017.06.038
[42] Grant DM, Pugmire RJ, Livingston RC, Strong KA, McMurry HL, Brugger RM. Methyl Libration in Propane Measured with Neutron Inelastic Scattering. Journal of Chemical Physics. 1970;52:4424-36. 10.1063/1.1673668
[43] Winnewisser M, Winnewisser BP, De Lucia FC, Tokaryk DW, Ross SC, Billinghurst BE. Pursuit of quantum monodromy in the far-infrared and mid-infrared spectra of NCNCS using synchrotron radiation. Physical Chemistry Chemical Physics. 2014;16:17373-407. 10.1039/C4CP01443J
[44] Western CM. PGOPHER: A program for simulating rotational, vibrational and electronic spectra. Journal of Quantitative Spectroscopy and Radiative Transfer. 2017;186:221-42. http://dx.doi.org/10.1016/j.jqsrt.2016.04.010
[45] Daunt SJ, Billinghurst BE, Flaud J-M, Lafferty W, Grzywacz R. First High Resolution IR Spectra of 2-^{13}C-Propane. The ν_9 B-Type Band Near 366.767 cm^{-1} and the ν_{26} C-Type Band Near 746.615 cm^{-1}. Determination Of Ground And Upper State Constants. International Symposium on Molecular Spectroscopy. Champaign-Urbana, Illinois 2017. 10.15278/isms.2017.FA04
[46] Kozlowski R, Kubica Z, Rzeszotarska B. A Simplified Synthesis of Lower Alkyl Bromides. Organic Preparations and Procedures International. 1988;20:177-80. 10.1080/00304948809355804
[47] Western CM, Daunt SJ, Grzywacz R, Lafferty WJ, Flaud J-M, Billinghurst BE, et al. First High Resolution Infrared Spectra of 2-^{13}C-Propane. doi:10.5523/bris.2igd3g8p8hvzj2coa2agm0cocd: University of Bristol Research Data Repository; 2020.
[48] Sharpe SW, Johnson TJ, Sams RL, Chu PM, Rhoderick GC, Johnson PA. Gas-Phase Databases for Quantitative Infrared Spectroscopy. Appl Spectrosc. 2004;58:1452-61. http://as.osa.org/abstract.cfm?URI=as-58-12-1452
[49] Kochanov RV, Gordon IE, Rothman LS, Shine KP, Sharpe SW, Johnson TJ, et al. Infrared absorption cross-sections in HITRAN2016 and beyond: Expansion for climate, environment, and atmospheric applications. Journal of Quantitative Spectroscopy and Radiative Transfer. 2019;230:172-221. https://doi.org/10.1016/j.jqsrt.2019.04.001
[50] Lafferty WJ, Flaud JM, Herman M. Resolved torsional splitting in the ν_{18} and ν_{19}- bands of propene. Journal of Molecular Structure. 2006;780-781:65-9. https://doi.org/10.1016/j.molstruc.2005.03.051
[51] Western CM, Billinghurst BE. Automatic and semi-automatic assignment and fitting of spectra with PGOPHER. Physical Chemistry Chemical Physics. 2019;21:13986-99. 10.1039/C8CP06493H
[52] Daunt SJ, Billinghurst BE, Grzywacz R. First High Resolution IR Study Of The ν_{14}(A') A-Type Band Near 421.847 cm^{-1} of 2-^{13}C-Propene. International Symposium on Molecular Spectroscopy. Champaign-Urbana, Illinois 2017. 10.15278/isms.2017.FA06
[53] Watson JKG. Determination of Centrifugal Distortion Constants of Asymmetric Top Molecues. Journal of Chemical Physics. 1967;46:1935-49.
[54] Drouin BJ, Pearson JC, Walters A, Lattanzi V. THz measurements of propane. J Mol Spectrosc. 2006;240:227-37. 10.1016/j.jms.2006.10.007
[55] Gjuraj D, Billinghurst BE, Flaud J-M, Lafferty W, Grzywacz R, Daunt SJ. First High Resolution IR Spectra of 2,2-D_2-Propane. The ν_{15} (B_1) A-Type Band Near 954.709 cm^{-1}. Determination of Ground and Upper State Constants. International Symposium on Molecular Spectroscopy. Champaign-Urbana, Illinois 2017. 10.15278/isms.2017.TK08
[56] Gjuraj D, Billinghurst BE, Flaud J-M, Lafferty W, Grzywacz R, Daunt SJ. First Far-IR Spectra of 2,2-D_2-Propane: The ν_9 (A_1) B-Type Band Near 365.3508 cm^{-1}. The Determination of Ground and Upper State Constants. International Symposium on Molecular Spectroscopy. Champaign-Urbana, Illinois 2018. 10.15278/isms.2018.WH11
[57] Gjuraj D, Billinghurst BE, Flaud J-M, Lafferty W, Grzywacz R, Daunt SJ. First High Resolution IR Spectra Of 1-^{13}C-Propane. The ν_9 B-Type Band Near 366.404 cm^{-1} and the ν_{26} C-Type Band Near 748.470 cm^{-1}. Determination of Ground And Upper State Constants. International Symposium on Molecular Spectroscopy. Champaign-Urbana, Illinois 2017. 10.15278/isms.2017.TK08
[58] Daunt SJ, Billinghurst BE, Flaud J-M, Lafferty W, Grzywacz R. First High Resolution IR Spectra of 2-D_1-Propane. The ν_9 (A_1) B-Type Band Near 367.2389 cm^{-1}. International Symposium on Molecular Spectroscopy. Champaign-Urbana, Illinois 2018. 10.15278/isms.2018.WH10
[59] Daunt SJ, Grzywacz R, Western C, Lafferty W, Flaud J-M, Hutchings R, et al. First High Resolution Infrared Spectra Of 1-D_1-Propane. First Analysis Of The ν_9 A_1 Type B Band Near 358 cm^{-1}. International Symposium on Molecular Spectroscopy. Champaign-Urbana, Illinois 2019. 10.15278/isms.2019.ML04